中国光学 Chinese Optics 核心期刊

双波长视网膜成像自适应光学系统的轴向色差补偿方法

朱沁雨 韩国庆 彭建涛 饶启龙 沈毅力 陈梅蕊 孙会娟 毛红敏 徐国定 曹召良 宣丽

Longitudinal chromatic aberration compensation method for dual-wavelength retinal imaging adaptive optics systems

ZHU Qin-yu, HAN Guo-qing, PENG Jian-tao, RAO Qi-long, SHEN Yi-li, CHEN Mei-rui, SUN Hui-juan, MAO Hong-min, XU Guo-ding, CAO Zhao-liang, XUAN Li

引用本文:
朱沁雨, 韩国庆, 彭建涛, 饶启龙, 沈毅力, 陈梅蕊, 孙会娟, 毛红敏, 徐国定, 曹召良, 宣丽. 双波长视网膜成像自适应光学系统的轴向色差补偿方法[J]. 中国光学, 2022, 15(1): 79-89. doi: 10.37188/CO.EN.2021-0009
ZHU Qin-yu, HAN Guo-qing, PENG Jian-tao, RAO Qi-long, SHEN Yi-li, CHEN Mei-rui, SUN Hui-juan, MAO Hong-min, XU Guo-ding, CAO Zhao-liang, XUAN Li. Longitudinal chromatic aberration compensation method for dual-wavelength retinal imaging adaptive optics systems[J]. *Chinese Optics*, 2022, 15(1): 79-89. doi: 10.37188/CO.EN.2021-0009

在线阅读 View online: https://doi.org/10.37188/CO.EN.2021-0009

您可能感兴趣的其他文章

Articles you may be interested in

双压电片镜在同步辐射光源光学系统中的应用

Application of bimorph mirror in the optical system of synchrotron radiation light source

中国光学. 2017, 10(6): 699 https://doi.org/10.3788/CO.20171006.0699

结构紧凑的双波长连续波掺铒光纤激光器

Compact dual-wavelength continuous-wave Er-doped fiber laser

中国光学. 2019, 12(4): 810 https://doi.org/10.3788/CO.20191204.0810

基于智能手机的眼底成像系统

Smartphone-based fundus imaging system

中国光学. 2019, 12(1): 97 https://doi.org/10.3788/CO.20191201.0097

采用色差先验约束的像差校正技术

Aberration correction technology based on chromatic aberration prior constraints

中国光学. 2018, 11(4): 560 https://doi.org/10.3788/CO.20181104.0560

用高斯光学和三级像差理论求变焦距物镜的初始解

Find preliminary solution of zoom objective lens using gaussian optics and third-order aberration theory

中国光学. 2018, 11(6): 1047 https://doi.org/10.3788/CO.20181106.1047

多尺度窗口的自适应透射率修复交通图像去雾方法

A traffic image dehaze method based on adaptive transmittance estimation with multi-scale window

中国光学. 2019, 12(6): 1311 https://doi.org/10.3788/CO.20191206.1311

文章编号 2095-1531(2022)01-0079-11

Longitudinal chromatic aberration compensation method for dual-wavelength retinal imaging adaptive optics systems

ZHU Qin-yu[1], HAN Guo-qing[2], PENG Jian-tao[3], RAO Qi-long[3], SHEN Yi-li[3], CHEN Mei-rui[1], SUN Hui-juan[4], MAO Hong-min[1], XU Guo-ding[1], CAO Zhao-liang[1*], XUAN Li[2]

(1. *Jiangsu Key Laboratory of Micro and Nano Heat Fluid Flow Technology and Energy Application*, *School of Physical Science and Technology*, *Suzhou University of Science and Technology*, *Suzhou* 215009, *China*;
2. *State Key Laboratory of Applied Optics*, *Changchun Institute of Optics*, *Fine Mechanics and Physics*, *Chinese Academy of Sciences*, *Changchun* 130033, *China*;
3. *Shanghai Institute of Satellite Engineering*, *China Aerospace Science and Technology Corporation*, *Shanghai* 201109, *China*;
4. *Institute of Mathematics and Physics*, *Institute of Fundamental and Interdisciplinary Sciences*, *Beijing Union University*, *Beijing* 100101, *China*)

* *Corresponding author*, *E-mail*: *caozl@usts.edu.cn*

Abstract: Dual-wavelength retinal imaging adaptive optics systems are suitable for high contrast and resolution imaging of retinal capillaries. The compensation of the Longitudinal Chromatic Aberrations (LCAs) in dual-wavelength adaptive systems is researched. The LCA is measured, the measured wavefronts are analyzed, and the arbitrary wavefront LCA compensation method is given. An adaptive correction experiment is carried out and the experimental results indicate that the root mean square error of the wavefront is reduced to 0.16 λ (λ=589 nm) and the retinal capillary resolution is improved to 6 μm. This work may be used for the clinical applications of retinal imaging.

Key words: adaptive optics; retinal imaging; longitudinal chromatic aberration; dual-wavelength

收稿日期:2021-09-06; **修订日期**:2021-09-26

基金项目:江苏省“十三五”重点学科 (No. 2016876); 中国航天科技集团公司第八研究院产学研合作基金资助(No. SAST2020-025); 北京联合大学学术研究项目 (No. ZK70202007)

Supported by China Jiangsu Key Disciplines of the Thirteenth Five-Year Plan (No. 20168765); Industry-University-Institute Cooperation Foundation of the Eighth Research Institute of China Aerospace Science and Technology Corporation (No. SAST2020-025); Academic Research Projects of Beijing Union University (No. ZK70202007).

双波长视网膜成像自适应光学系统的轴向色差补偿方法

朱沁雨[1], 韩国庆[2], 彭建涛[3], 饶启龙[3], 沈毅力[3], 陈梅蕊[1],
孙会娟[4], 毛红敏[1], 徐国定[1], 曹召良[1*], 宣　丽[2]
(1. 苏州科技大学 物理科学与技术学院 江苏微纳热流技术与能源应用重点实验室, 江苏 苏州 215009;
2. 中国科学院 长春光学精密机械与物理研究所 应用光学国家重点实验室, 长春 130033;
3. 中国航天科技集团公司上海卫星工程研究所, 上海 201109;
4. 北京联合大学 基础与交叉科学研究所 数学与物理研究所, 北京 100101)

摘要: 双波长视网膜成像自适应光学系统非常适用于视网膜微血管的高对比度和高分辨率成像。本文重点研究了双波长自适应系统的轴向色差补偿问题。首先对轴向色差进行了测量, 对实测波前进行了分析, 并给出任意波前轴向色差补偿法。自适应校正实验结果显示, 色差补偿后, 波前均方根误差减小到 0.16 λ(λ=589 nm), 视网膜微血管分辨率提高到 6 μm。这项工作可用于视网膜成像的临床应用。

关　键　词: 自适应光学; 视网膜成像; 轴向色差; 双波长
中图分类号: O439　　**文献标志码:** A　　**doi:** 10.37188/CO.EN.2021-0009

1 Introduction

Adaptive Optics Systems (AOSs) have been widely used for retinal imaging to obtain high resolution images of photoreceptor mosaics and retinal capillaries[1-8]. High resolution retinal images can enable the early diagnosis of numerous ocular and systemic diseases, such as glaucoma[9], age-related macular degeneration[7], and diabetes[6]. Human eyes are highly sensitive to visible light; thus, the infrared waveband is used for wavefront detection and longtime imaging of the retina. Therefore, almost all the AOSs utilize near-infrared light to detect aberrations and obtain high resolution images of the photoreceptor cells using the high reflectivity in the near-infrared waveband. However, high contrast images of retinal capillaries can only be acquired at the visible (530−580 nm) waveband[10-12]. Moreover, in contrast to the adaptive correction imaging of photoreceptor cells, tracing and positioning the capillary must be done many times to obtain their images. In this process, the detection and correction of the wavefront and the retina imaging should be performed for every instance of tracking. Infrared light is suitable for this. After the capillary is positioned accurately, the imaging light is switched to use visible light and the high contrast image of the capillary is achieved. Consequently, the dual-wavelength AOS is needed for high-resolution retinal imaging: near-infrared light is used to trace and position the capillary, detect aberrations and observe photoreceptor cells, and visible light is used to produce high-contrast images of the capillaries. Furthermore, multi-wavelength AOS is used to get more information on retinal features (the nerve fiber layer, capillary, and choroid) and improve the contrast of the image[13-14]. As the wavelength used for retinal imaging is different to that used for aberration detection, the Longitudinal Chromatic Aberration (LCA) must be considered when acquiring high-resolution images of the retina.

Newton first described the LCA of the human

eye hundreds of years ago[15]. Then, researchers measured the LCA of the human eye using different wavelengths[16-22]. They mainly focused on the effect of the LCA on the power of the eye, which was used to design intraocular lenses in cataract surgery. Recently, the compensation methods of LCA were studied with achromatizing lens[23-24], moving the imaging camera or the light source[14,25], and using a filter-based Badal compensator[26]. The first two methods cannot compensate for the LCA accurately due to inter-subject variability and the little misalignment of the lens. The filter-based Badal compensator may compensate for the LCA conveniently in a multi-wavelength optical system. However, the control operation of Badal is complicated and only the defocus is compensated. In the paper, we propose a simple method to compensate for the LCA in dual-wavelength retina imaging AOS. Based on this method, we hope to realize high-resolution retinal capillaries imaging with high-contrast. The concrete work includes: (1) LCA measurement, (2) LCA compensation method, and (3) application of LCA compensation in AOs imaging of retinal capillaries.

2 Longitudinal chromatic aberration measurement

2.1 Optical layout

To compensate for the LCA, the AOS should be first measured and analyzed. An optical setup was established in the laboratory, as shown in Fig. 1. Two lasers with wavelengths of 589 and 808 nm were selected as the dual-wavelength optical sources. The collimated beam is reflected to the eye by BS3 and focused on the retina, then reflected out from the eye. The spatial coherence of the laser was decreased by the diffuser to reduce the speckle artifacts. An annular aperture was placed at the conjugated plane of the pupil to eliminate the reflected light from the cornea. The light reflected from the retina passed through L7 and L8 and went into a Shack Hartmann wavefront sensor (SH-WFS) for wavefront detection. The SH-WFS, fabricated in-house, had a microlens array of 20×20, was 3 mm in diameter, and had an acquistition frequency of 515 Hz. A pupil camera was used to acquire the correct position of the pupil. A target illuminated by LED was used for fixation.

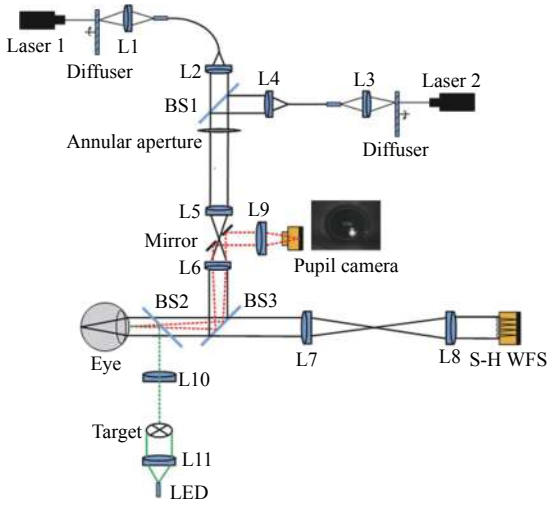

Fig. 1　Illustration of the optical setup for LCA measurement: two lasers are used with the wavelength of 589 nm and 808 nm

The LCA is the difference between two wavefronts acquired at two different wavelengths. Ocular aberration does not change within 50 ms [27]. Hence, the aberration should be measured immediately for the two wavelengths. To simultaneously measure the dual-wavelength ocular aberrations, two lasers and SH-WFS are controlled with a certain time sequence, as shown in Fig. 2. The exposure time of the SH-WFS is set to 3 ms to measure the wavefront accurately, and the total time delay is 10 ms. While giving a start signal, laser 1 and the SH-WFS are triggered simultaneously, laser is turned on with 3 ms for wavefront detection and the ocular aberration can then be measured at 808-nm wavelength. With a time delay of 10 ms, laser 2 and SH-WFS are triggered simultaneously and then the ocular aberration is measured again at 589-nm wavelength. Thus, the ocular aberrations are repres-

ented as instances with no change and the difference between the two measured wavefronts of the dual-wavelength are the LCA.

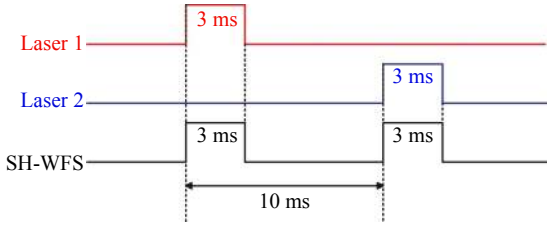

Fig. 2 Time sequence for system control

2.2 Measured results

Five subjects, between the ages of 24 and 28, with healthy eyes with myopia with degrees from 100 to 500, were selected as subjects to measure the LCA. A wavelength of 589 nm was used to image their retinal capillaries; thus, all the aberrations were expressed with λ=589 nm. Fig.3 (Color online) shows the measured wavefronts of subject A. The LCA was obtained by subtracting the aberration of 808 nm from the aberration of 589 nm and its Root Mean Square (RMS) value was 1.3 λ, as shown in Fig. 3(c). Fig. 3(d) shows the LCA without the defocus and its RMS value is 0.31 λ, which corresponds to 6 times the diffraction limit. Therefore, although the defocus is the main component of LCA, the system must compensate for the residual LCA to acquire high-resolution images of the retina. The LCAs of different subjects are shown in Fig.4. The magnitudes of the LCA of other subjects are similar to that of subject A. The defocus can be overcome by moving the imaging camera; thus, we only consider the compensation of LCA without the defocus in the following.

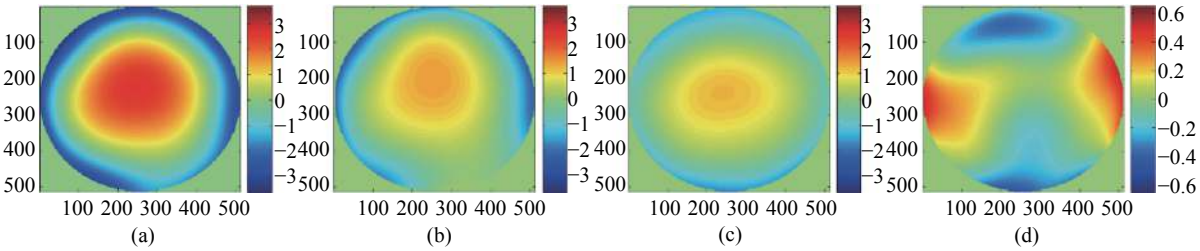

Fig. 3 Measured wavefronts of subject A. (a) Wavelength of 589 nm; (b) wavelength of 808 nm; (c) LCA; (d) LCA without defocus

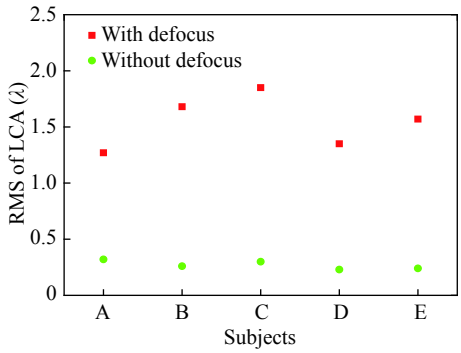

Fig. 4 Measured LCA for different subjects, with and without defocus at λ=589 nm

3 Arbitrary wavefront LCA compensation method

For the dual-wavelength retinal imaging of the AOS, the aberration was detected at the 808 nm wavelength and corrected with the wavefront corrector (WFC). A light source with a wavelength of 589 nm was used for retinal capillary imaging and the LCA was produced and should be corrected by the WFC simultaneously and the LCA should be detected and added to the aberration detected at 808 nm. The LCA of the eye varies slowly; thus, it should be measured and selected correctly for effective compensation. Consequently, the variation of LCA with time should be considered first. We measured the LCA of subject A at time intervals of 5 minutes, 1 hour, 10 hours, 15 hours, 24 hours, 30 hours, and 36 hours, as shown in Fig. 5 (Color online). The wavefronts are similar to a certain extent, but the LCA changes at different times. The RMS of

LCA as a function of the time is shown in Fig.6. It indicates that the RMS of LCA changes minimally with time. The mean value and standard deviation of LCA are 0.32 λ and 0.032 λ, respectively.

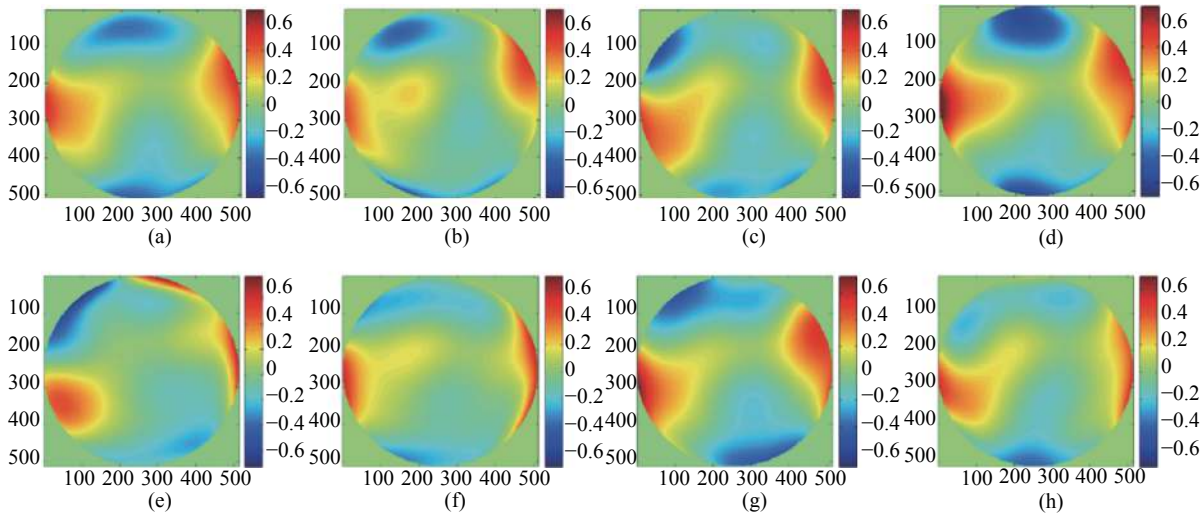

Fig. 5　Wavefronts of LCA at different times for subject A. (a) Start; (b) 5 minutes later; (c) 1 hour later; (d) 10 hours later; (e) 15 hours later; (f) 24 hours later; (g) 30 hours later; (h) 36 hours later

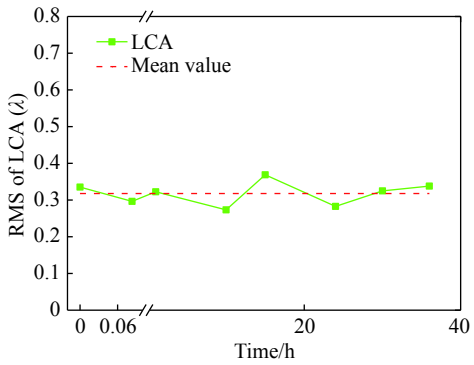

Fig. 6　Measured LCA at different times for subject A

Because the wavefronts of LCA measured at different times have a certain similarity (shown in Fig.5) and the RMS value of LCA almost has no change (shown as Fig. 6), we select the wavefront of aberration measured at an arbitrary time to represent the timely detected LCA. Thus, before adaptive correction, the LCA should be measured first; then, while the adaptive correction is started, the measured LCA is combined into the real-time detected aberration and will be corrected by the WFC. Hence, after adaptive correction, the residual of LCA may be calculated with:

$$LCA_{\text{residual}} = LCA_{\text{measured}} - LCA_{\text{arbitrary}} \quad . \qquad (1)$$

Which we call the arbitrary wavefront method. To simulate the correction effect of LCA, the first wavefront in Fig. 5 was selected as the arbitrary wavefront and the compensation results are shown in Fig. 7 (Color online). It is shown that, after compensation, the RMS value of the residual light is between 0.13 λ and 0.18 λ, the mean value of the LCA is 0.16 λ with a standard deviation of 0.017 λ.

By following the same process, other wavefronts in Fig. 5 were chosen successively as the arbitrary wavefront and the mean value of the RMS of residual are shown in Fig. 8. It indicates that after compensation, the mean RMS of LCA decreased from 0.3 λ to about 0.15 λ. The mean RMS of LCA at different times was averaged again and the computed result shows that, the averaged RMS of LCA is decreased to 0.158±0.011 λ. The LCA compensations of other subjects were computed and their mean values are shown in Fig. 9. It indicates that, after compensation, the mean RMS values of LCA are reduced to 0.166±0.017 λ for different subjects. Consequently, the arbitrary wavefront compensation method is a simple and effective method of compensating for LCA in a dual-wavelength AOS.

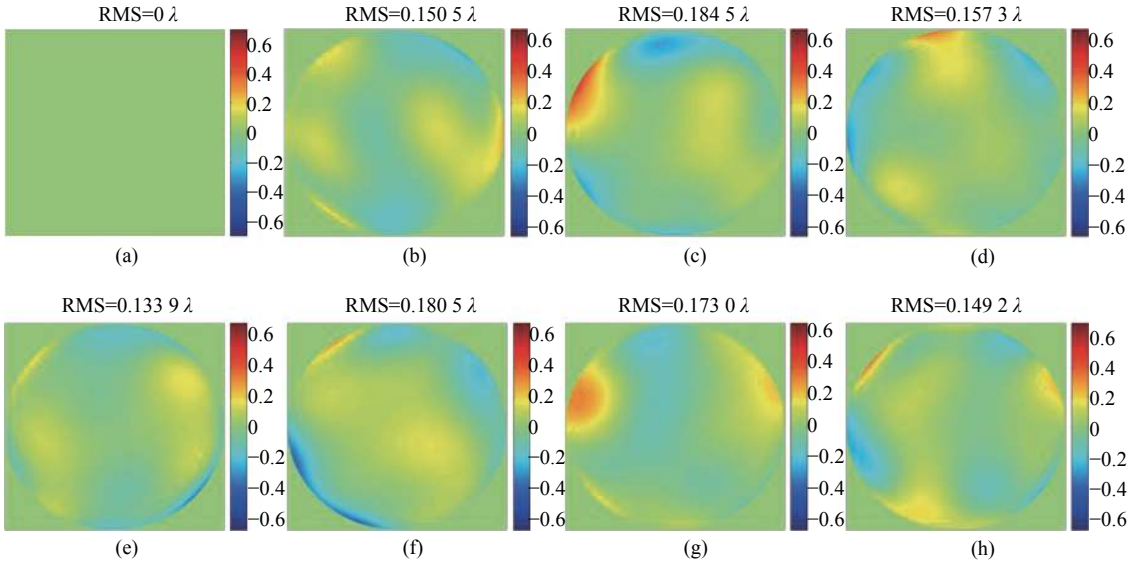

Fig. 7 Calculated compensation of LCA for subject A at different times while the first wavefront of Fig. 5 is chosen as the arbitrary wavefront. The mean value of LCA is 0.16 λ with the standard deviation of 0.017. (a) Start; (b) 5 minutes later; (c) 1 hour later; (d) 10 hours later; (e) 15 hours later; (f) 24 hours later; (g) 30 hours later; (h) 36 hours later

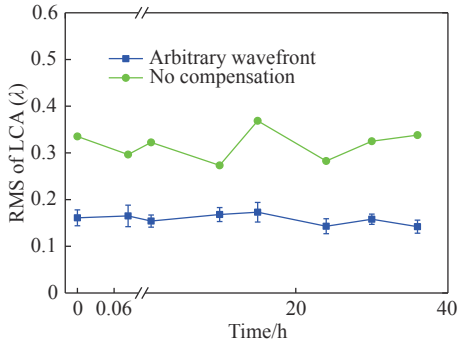

Fig. 8 Compensation of LCA for subject A at different times. The mean value of the arbitrary wavefront is 0.158±0.011 λ.

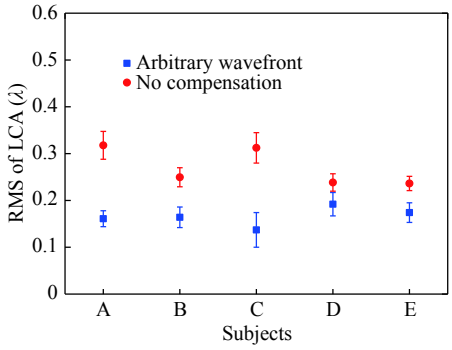

Fig. 9 Compensation of LCA for different subjects. The mean values of the arbitrary wavefront is 0.166± 0.017 λ.

4 LCA compensation experiment

To validate the arbitrary wavefront compensation method of LCA, an AOS was built, as shown in Fig. 10 (Color online), and mainly consists of the illumination, aberration correction and imaging, pupil monitoring, and target fixation. The illumination system included two lasers (CNI Inc.) with wavelengths of 589 and 808 nm, which were used for imaging the retinal capillaries and for wavefront detection. An annular aperture was placed at the conjugated position of the pupil to eliminate the reflected light from the cornea. The incidence optical power was lower than the maximum permissible exposure of the ANSI[28-30]. With the diameter of illumination area being 250 μm, the MPEs of 589 nm and 808 nm are 2 mW and 15 mW respectively. For the safety of the subjects′ eyes, powers of 589 nm and 808 nm are selected with 50 μW and 300 μW, respectively. The aberration was detected using an SH-WFS which is the same as that used for the LCA detection. A liquid crystal wavefront corrector (LC-WFC) (BNS, HSP256-0785) was utilized to correct the aberration with 256 pixel×256 pixel, 6.14 mm× 6.14 mm aperture, and a frequency of 500 Hz. The corrected beam goes to an imaging camera that can be axially moved using an electrically controlled translation stage. The pupil position is observed by a pupil camera (DVC, DVC-710M), which has 768 pixel×484 pixel, and pixels of 8.4 μm×9.8 μm in

size, and a 65 dB signal-to-noise ratio. The target staring system is used to control the illumination position of the retina. A Complementary Metal Oxide Semiconductor (COMS) camera (ANDOR, Zyla 5.5) of 2 560 pixel×2 160 pixel, each being 6.5 μm in size, and having 60% QE, and a 100 Hz frame rate is used for retinal capillary imaging. To improve the energy utilization ratio of the optical system, an open-loop adaptive optics scheme was chosen for the aberration correction and imaging system, whose detailed information is described in Ref.[31]. Fig. 11 (Color online) shows the optical layout of the retinal adaptive correction and imaging system established on an optical flat.

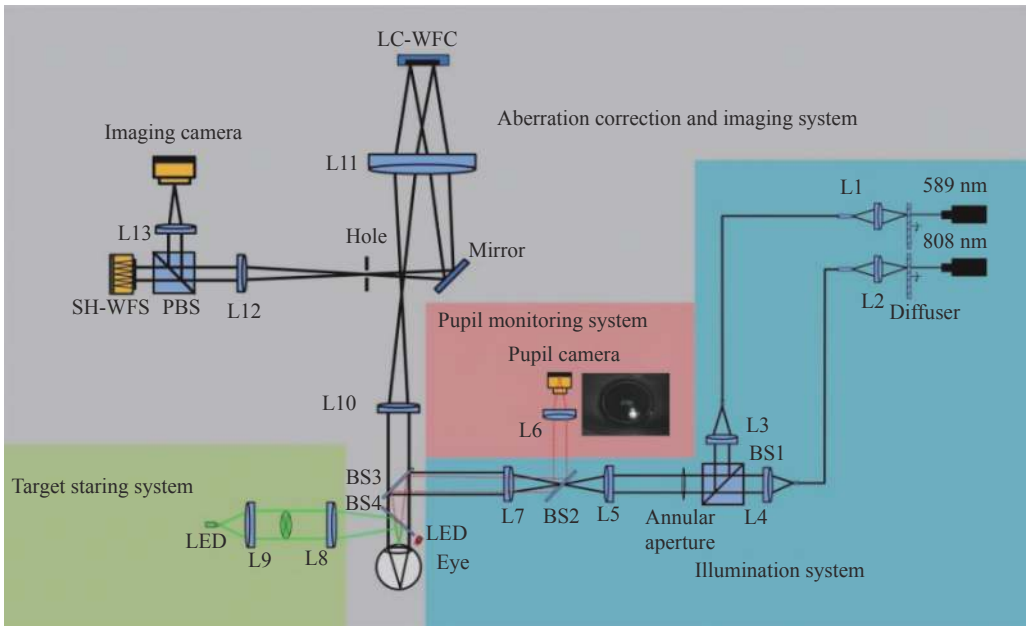

Fig. 10　Optical layout for the retinal imaging AOS: L1-L13, Lens 1- Lens 13; PBS, polarizing beam splitter; BS, beam splitter; an 808 nm laser is used for wavefront detection, tracing and positioning the capillary; a 589 nm laser is used for high contrast imaging of the capillary; the collimated beam comes from the illumination system and is reflected into the eye, and then reflected again out from the eye by the retina; this reflected light is detected and corrected by the adaptive optics system and imaged with an imaging camera; the pupil position is observed by the pupil monitoring system and the eye is fixed with the target staring system

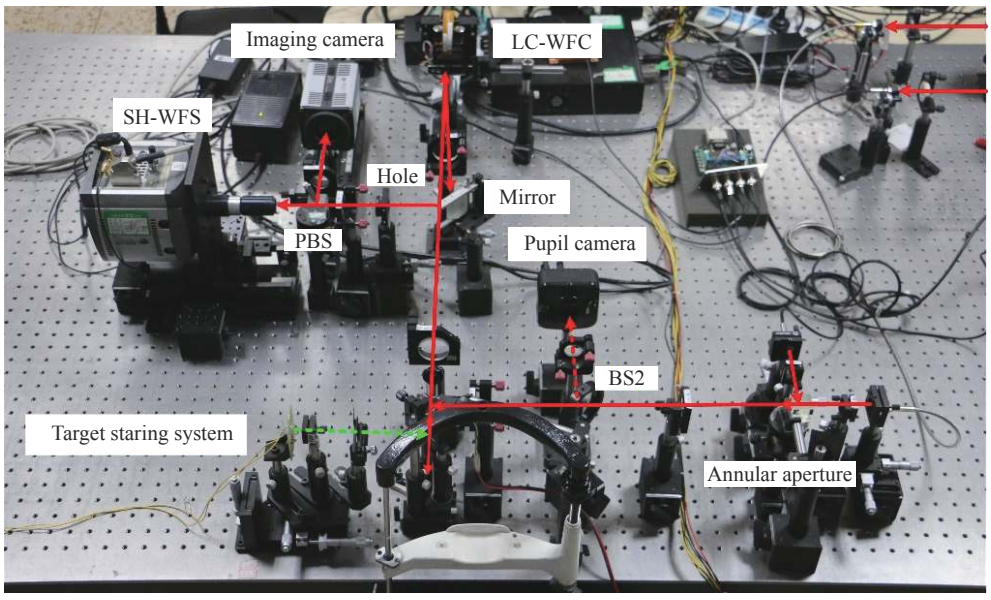

Fig. 11　Experimental configuration of the AOS on an optical flat

First, the LCA was measured with the method described in Section 2. Then, an adaptive correction experiment was performed with the compensation of the LCA. To do the comparison, an adaptive correction was done without the compensation of LCA. A Field Of View (FOV) of 250 μm was selected for retinal imaging, and the resolution of the optical system was approximately evaluated with the diameter of the capillary[32-33]. Fig. 12 (Color online) shows the experimental results for subjects A and C. It indicates that, before correction, the aberrations of subjects A and C were 1.68 λ (Fig. 12(a)) and 1.71 λ (Fig. 12(e)), respectively, which were detected at the 808 nm wavelength. Adaptive correction was performed without LCA compensation and the distortions were reduced to 0.31 λ (Fig. 12(b)) and 0.307 λ (Fig. 12(f)), for subjects A and C, respectively. Moreover, the resolutions of the retinal capillaries were 13 μm (Fig. 12 (c)) and 14 μm (Fig. 12 (g)), for subjects A and C, respectively. With a pupil diameter of 6 mm, the diffraction-limited resolution was 2.2 μm at a wavelength of 589 nm. Consequently, the image resolution decreased by 6 times the diffraction limit for RMS=0.31 λ. Thus, the image resolution should be 13.2 μm, which was compatible with the size of the retinal capillaries shown in Figs. 12 (c) and 12 (g). Then, the LCAs were counteracted and aberrations of subjects A and C decreased to approximately 0.16 λ and 0.15 λ, respectively, according to the calculated results in Fig. 8. The resolutions of the retinal capillaries were improved to 6 μm (Fig. 12 (d)) and 7 μm (Fig. 12 (h)) after LCA compensation. Theoretically, the image resolutions should be improved to 1.7 and 1.5 times the diffraction limit and 4 μm and 3 μm retinal capillaries will be resolved, which corresponds to subjects A and C. The retinal capillaries with sizes of 6 μm and 7 μm were observed for subjects A and C. We think that this is caused by actual capillary size but not correction accuracy. Of course, for the other three subjects, similar results were obtained too. Therefore, using the LCA compensation method, the image resolution can be greatly improved for the dual-wavelength adaptive correction system and a resolution of 4 μm may be acquired. The retinal capillary size is approximately 5 μm; thus, LCA compensation is valid for clinical applications.

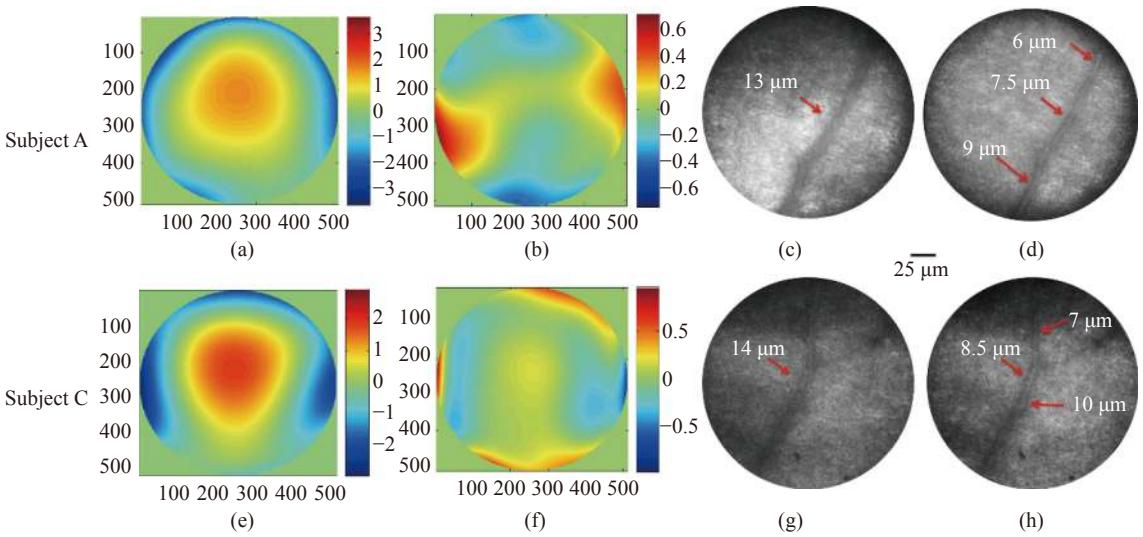

Fig. 12 Experiment results of adaptive correction and LCA compensation for subjects A and C. (a) Measured aberration at 808 nm for subject A; (b) wavefront of LCA for subject A; (c) image of retinal capillary without LCA compensation for subject A; (d) image of retinal capillary after LCA compensation for subject A; (e) measured aberration at 808 nm for subject C; (f) wavefront of LCA for subject C; (g) image of retinal capillary without LCA compensation for subject C; (h) image of retinal capillary after LCA compensation for subject C

5 Conclusion

An LCA compensation method is proposed for a dual-wavelength retinal imaging adaptive optics system. First, the LCAs of the human eye were measured in 5 subjects. An optical setup was established in the laboratory with dual wavelengths of 589 and 808 nm. The measured results showed that the RMS of LCA without defocus was 0.31 λ or so. Then, subject A was chosen as an example for the analysis. The LCA of subject A was measured at different times and results showed that its RMS changed minimally with time and the wavefronts of LCA measured at different times showed similarities. Hence, arbitrary wavefronts were selected as the aberrations to do the compensation. Calculated compensation results indicated that the LCA is reduced from 0.32 λ to 0.158 λ. Moreover, the comparison was performed for different subjects and the results showed that the mean RMS values of LCA are reduced to 0.166±0.017 λ for different subjects.

At last, an adaptive correction experiment was done for two subjects using the arbitrary wavefront LCA compensation method. The results showed that with LCA compensation, the RMS error of the wavefront decreased from 0.31 λ to approximately 0.16 λ. The resolutions of the retinal capillaries were improved from 13 μm and 14 μm to 6 μm and 7 μm for subjects A and C, respectively. Therefore, the LCA may be counteracted effectively with the proposed method. Furthermore, the proposed method may be applied to multi-wavelength retinal imaging AOS as well. This work is helpful for the LCA compensation of multi-wavelength retinal imaging AOS and acquiring high-resolution and high-contrast retinal images for clinical applications.

References:

[1] LIANG J ZH, WILLIAMS D R, MILLER D T. Supernormal vision and high-resolution retinal imaging through adaptive optics[J]. *Journal of the Optical Society of America A*, 1997, 14(11): 2884-2892.

[2] ROORDA A, WILLIAMS D R. The arrangement of the three cone classes in the living human eye[J]. *Nature*, 1999, 397(6719): 520-522.

[3] JONNAL R S, RHA J, ZHANG Y, *et al*.. *In vivo* functional imaging of human cone photoreceptors[J]. *Optics Express*, 2007, 15(24): 16141-16160.

[4] LI K Y, ROORDA A. Automated identification of cone photoreceptors in adaptive optics retinal images[J]. *Journal of the Optical Society of America A*, 2007, 24(5): 1358-1363.

[5] DUBRA A, SULAI Y, NORRIS J L, *et al*.. Noninvasive imaging of the human rod photoreceptor mosaic using a confocal adaptive optics scanning ophthalmoscope[J]. *Biomedical Optics Express*, 2011, 2(7): 1864-1876.

[6] CHUI T Y P, VANNASDALE D A, BURNS S A. The use of forward scatter to improve retinal vascular imaging with an adaptive optics scanning laser ophthalmoscope[J]. *Biomedical Optics Express*, 2012, 3(10): 2537-2549.

[7] ZAYIT-SOUDRY S, DUNCAN J L, SYED R, *et al*.. Cone structure imaged with adaptive optics scanning laser ophthalmoscopy in eyes with nonneovascular age-related macular degeneration[J]. *Investigative Ophthalmology & Visual Science*, 2013, 54(12): 7498-7509.

[8] QUERQUES G, KAMAMI-LEVY C, GEORGES A, *et al*.. Appearance of regressing drusen on adaptive optics in age-related macular degeneration[J]. *Ophthalmology*, 2014, 121(2): 611-612.

[9] PAQUES M, BROLLY A, BENESTY J, *et al*.. Venous nicking without arteriovenous contact: the role of the arteriolar microenvironment in arteriovenous nickings[J]. *JAMA Ophthalmology*, 2015, 133(8): 947-950.

[10] MARTIN J A, ROORDA A. Direct and noninvasive assessment of parafoveal capillary leukocyte velocity[J]. *Ophthalmology*, 2005, 112(12): 2219-2224.

[11] HAN G Q. *High contrast imaging study of retinal capillaries in human eyes*[D]. Beijing: Changchun Institute of Optics, Fine Mechanics and Physics University of Chinse Academy of Sciences, 2018: 28-30. (in Chinese)

[12] FABER D J, AALDERS M C G, MIK E G, *et al*.. Oxygen saturation-dependent absorption and scattering of blood[J].

Physical Review Letters, 2004, 93(2): 028102.

[13] REINHOLZ F, ASHMAN R A, EIKELBOOM R H. Simultaneous three wavelength imaging with a scanning laser ophthalmoscope[J]. *Cytometry Part A*, 1999, 37(3): 165-170.

[14] GRIEVE K, TIRUVEEDHULA P, ZHANG Y H, *et al*.. Multi-wavelength imaging with the adaptive optics scanning laser ophthalmoscope[J]. *Optics Express*, 2006, 14(25): 12230-12242.

[15] NEWTON S I. *Opticks, or, A Treatise of the Reflections, Refractions, in Flections & Colours of Light*[M]. 4th ed. London: G. Bell & Sons, Ltd. , 1931.

[16] WALD G, GRIFFIN D R. The change in refractive power of the human eye in dim and bright light[J]. *Journal of the Optical Society of America*, 1947, 37(5): 321-336.

[17] THIBOS L N, BRADLEY A, STILL D L, *et al*.. Theory and measurement of ocular chromatic aberration[J]. *Vision Research*, 1990, 30(1): 33-49.

[18] FERNÁNDEZ E J, ARTAL P. Ocular aberrations up to the infrared range: from 632.8 to 1070 nm[J]. *Optics Express*, 2008, 16(26): 21199-21208.

[19] RUCKER F J, OSORIO D. The effects of longitudinal chromatic aberration and a shift in the peak of the middle-wavelength sensitive cone fundamental on cone contrast[J]. *Vision Research*, 2008, 48(19): 1929-1939.

[20] NAKAJIMA M, HIRAOKA T, HIROHARA Y, *et al*.. Verification of the lack of correlation between age and longitudinal chromatic aberrations of the human eye from the visible to the infrared[J]. *Biomedical Optics Express*, 2015, 6(7): 2676-2694.

[21] VINAS M, DORRONSORO C, CORTES D, *et al*.. Longitudinal chromatic aberration of the human eye in the visible and near infrared from wavefront sensing, double-pass and psychophysics[J]. *Biomedical Optics Express*, 2015, 6(3): 948-962.

[22] VINAS M, DORRONSORO C, GARZÓN N, *et al*.. In vivo subjective and objective longitudinal chromatic aberration after bilateral implantation of the same design of hydrophobic and hydrophilic intraocular lenses[J]. *Journal of Cataract & Refractive Surgery*, 2015, 41(10): 2115-2124.

[23] CHONG S P, ZHANG T W, KHO A, *et al*.. Ultrahigh resolution retinal imaging by visible light OCT with longitudinal achromatization[J]. *Biomedical Optics Express*, 2018, 9(4): 1477-1491.

[24] ZAWADZKI R J, CENSE B, ZHANG Y, *et al*.. Ultrahigh-resolution optical coherence tomography with monochromatic and chromatic aberration correction[J]. *Optics Express*, 2008, 16(11): 8126-8143.

[25] DUBRA A, SULAI Y. Reflective afocal broadband adaptive optics scanning ophthalmoscope[J]. *Biomedical Optics Express*, 2011, 2(6): 1757-1768.

[26] JIANG X Y, KUCHENBECKER J A, TOUCH P, *et al*.. Measuring and compensating for ocular longitudinal chromatic aberration[J]. *Optica*, 2019, 6(8): 981-990.

[27] ZHENG X L, LIU R X, XIA M L, *et al*.. Temporal properties study of ocular wave aberrations with high frequency sampling[J]. *Chinese Optics*, 2014, 34(7): 0733001.

[28] MORGAN J I W, HUNTER J J, MASELLA B, *et al*.. Light-induced retinal changes observed with high-resolution autofluorescence imaging of the retinal pigment epithelium[J]. *Investigative Ophthalmology & Visual Science*, 2008, 49(8): 3715-3729.

[29] DELORI F C, WEBB R H, SLINEY D H. Maximum permissible exposures for ocular safety (ANSI 2000), with emphasis on ophthalmic devices[J]. *Journal of the Optical Society of America A*, 2007, 24(5): 1250-1265.

[30] Laser Institute of America. ANSI Z136.1-2014 American national standard for safe use of lasers[S]. Orlando: American National Standards Institute, 2007: 22-29.

[31] LI CH, XIA M L, MU Q Q, *et al*.. High-precision open-loop adaptive optics system based on LC-SLM[J]. *Optics Express*, 2009, 17(13): 10774-10781.

[32] YANG L B, HU L F, LI D Y, *et al*.. Determining the imaging plane of a retinal capillary layer in adaptive optical imaging[J]. *Chinese Physics B*, 2016, 25(9): 094219.

[33] BURNS S A, ELSNER A E, CHUI T Y, *et al*.. *In vivo* adaptive optics microvascular imaging in diabetic patients without clinically severe diabetic retinopathy[J]. *Biomedical Optics Express*, 2014, 5(3): 961-974.

Author Biographics:

ZHU Qin-yu (1997 —), male, born in Wuxi, Jiangsu Province, master student. He received his bachelor's degree from Changshu Institute of Technology in 2019. He is mainly engaged in the research of photoelectric instruments and intelligent detection technology. E-mail: zhuqywx@163.com

朱沁雨(1997 —),男,江苏无锡人,硕士研究生,2019 年于常熟理工学院获得学士学位,主要研究方向为光电仪器与智能检测技术。 E-mail: zhuqywx@163.com

CAO Zhao-liang (1974—), male, born in Jiyuan, Henan Province, Ph.D., professor and doctoral supervisor. He received his Ph.D. from Changchun Institute of Optics, Fine Mechanics and Physics, Chinese Academy of Sciences in 2008. He is mainly engaged in research of liquid crystal adaptive optical system: optical design, optical experiment, theoretical analysis and simulation. E-mail: caozl@usts.edu.cn

曹召良(1974—),男,河南济源人,博士,教授,博士研究生导师,2008 年于中国科学院长春光学精密机械与物理研究所获得博士学位,主要从事液晶自适应光学系统:光学设计、光学实验以及理论分析和模拟工作。 E-mail: caozl@usts.edu.cn

《光学 精密工程》(月刊)

- 中国光学开拓者之一王大珩院士亲自创办的新中国历史最悠久的光学期刊
- 现任主编为国家级有突出贡献的青年科学家曹健林博士
- Benjamin J Eggleton, John Love 等国际著名光学专家为本刊国际编委

《光学 精密工程》主要栏目有现代应用光学(空间光学、纤维光学、信息光学、薄膜光学、光电技术及器件、光学工艺及设备、光电跟踪与测量、激光技术及设备);微纳技术与精密机械(纳米光学、精密机械);信息科学(图像处理、计算机应用与软件工程)等。

* 美国工程索引 EI 核心期刊
* 中国出版政府奖期刊提名奖
* 中国精品科技期刊
* 中文核心期刊
* 百种中国杰出学术期刊
* 中国最具国际影响力学术期刊

主管单位:中国科学院
主办单位:中国科学院长春光学精密机械与物理研究所
　　中国仪器仪表学会
地址:长春市东南湖大路 3888 号　　邮编:130033
电话:0431-86176855　　传真:0431-84613409
电邮:gxjmgc@ sina. com　　网址:http://www. eope. net
定价:100.00 元/册